Synchronous Reluctance Machine with Magnetically-Coupled, Double Three-Phase Windings

A.S.O. Ogunjuyigbe*, E.S. Obe**, D.V. Nicolae* and A.A. Jimoh*
* Department of Electrical Engineering, Tshwane University of Technology, Pretoria, South Africa
** Department of Electrical Engineering, University of Nigeria, Nsukka, Nigeria

***Abstract*—This paper presents the use of magnetically-coupled, double three-phase windings to improve the performance characteristics of synchronous reluctance machine with a simple salient rotor. This machine with both three windings housed in the same stator structure has the main winding connected to the main supply and the auxiliary connected to balanced capacitance for leading current injection. The power factor and torque performance characteristics of the machine with the scheme were investigated using the electromagnetic field and coupled circuit concepts and it is shown to have a desirable characteristics. The influence of the capacitor in energy conversion were also examined, the nature of the airgap flux distribution were determined and net flux of the machine with the scheme is shown to be sinusoidal.**

I. INTRODUCTION

The concept of multiple winding sets in machines can be traced to publications in the 1900's [1, 2]. In particular, dual winding machines; equipped with two winding sets have been considered for various motoring and generating applications, in view of the fact that, the two stator winding sets offer the possibility of more flexible energy conversion. For instance, energy can be transferred not only between stator and rotor like what is found in single winding machines, but also indirectly between stator winding sets.

Generally, multi-winding machines have been categorized as either 'split-wound' or 'self-cascaded' [3]. The "self-cascaded machine" was introduced by Hunt in 1907 [2]. It has two stator winding sets with different pole numbers, the same number of phases and sharing the same stator core. It requires a special rotor structure that has nested loops on the rotor to account for the effects of cascade connection [1, 3]. The special rotor structure is a major drawback for this machine type as the cost of the machine is increased and the efficiency is relatively low. However, it has potential utility in drive applications with a narrow speed range.

The split wound machine consists of two similar but separate windings wound for the same number of poles. It was introduced as a means to increase the power capability of large alternators, overcome the limitation imposed by the fault current interrupting capacity of circuit breakers [4, 5], and to permit electrical segregation of bus sections in large stations [6]. In recent past, the split wound machine concepts was used as a source of both regulated DC and AC output voltages [4, 6-8]. Drives based on these winding arrangements have improved torque and MMF characteristics.

This work therefore extend the advantages of the split wound machine concepts and capacitance injection to synchronous reluctance machine with simple salient rotor, so as to achieve an improved power factor and torque performance. Machine of similar structure has been discussed in [9, 10].

In this paper, an attempt, using the electromagnetic field concepts, at understanding the principle of operation of synchronous reluctance machine with magnetically coupled, double 3-φ stator windings and capacitance injection is reported. In section III, the electromagnetic field analysis concepts is used to determine the MMF distribution and stored energies, which are subsequently used to determine the electromagnetic torques developed [11, 12]. The equations that describe the airgap flux density distribution were developed from the first principle in section IV. Section V used the coupled circuit approach and an approximate equivalent circuit to investigate the impact of this machine topology on the torque and power factor performance of conventional synchronous reluctance machine. Conclusions were then drawn in section VI.

II. STATOR AND ROTOR CONFIGURATIONS OF THE EXPERIMENTAL MACHINE

The analysis set forth in this paper applies to synchronous reluctance machine with simple salient rotor having p poles. The machine is modified along the split wound machine concepts to accommodate two three-phase stator winding sets- main (*abc)* and auxiliary (*xyz*), and capacitance injection through the auxiliary winding. The two windings *abc* and *xyz* have same number of poles p, shares the same magnetic structure; occupying the same stator slots, thus, they are magnetically coupled while maintaining an electrical isolation between them. The main winding *abc* carry the load current, while the auxiliary *xyz* are directly connected to a balanced capacitor for leading current injection. The conceptual diagram of such arrangements is illustrated in Fig. 1. The capacitor attached to the auxiliary winding makes a leading current to be injected into the machine, such that the power factor, torque, torque per ampere, and the harmonic content of the

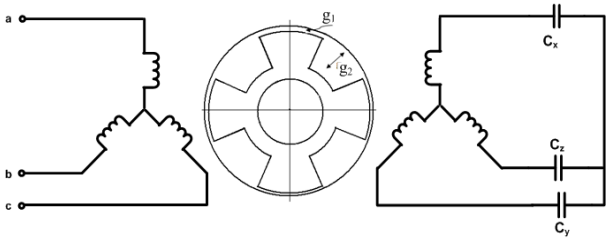

Fig. 1: Stator and rotor structure of the experimental machine

line current, of the machine is improved. This unique contribution, cumulated with the simplicity and the low manufacturing cost of the simple salient rotor construction, will make this machine topology attractive as a potential means of high speed, synchronous drive, particularly in areas where arcing within the machine structure is not allowed.

III. ELECTROMAGNETIC TORQUE

In the analysis that follows, classical assumptions were made to obtain closed form equations [13, 14], thus, only the fundamental components of the stator winding distributions, stator currents and voltages are considered. These are sufficient enough to explain the fundamental operation of the machine.

The fundamental component of the winding distributions of windings *abc* and *xyz* is expressed as

$$N_k(\theta) = N_{sj}\cos(p\theta - \varphi_k) \tag{1}$$

If j=1, k = a,b,c; $\varphi_a=\varphi_1$; $\varphi_b = \varphi_1 - 2\pi/3$ and $\varphi_b = \varphi_1 - 4\pi/3$
If j=2, k = x,y,z; $\varphi_x=\varphi_2$; $\varphi_y = \varphi_2 - 2\pi/3$ and $\varphi_z = \varphi_1 - 4\pi/3$

The angle θ is the circumferential angle of the stator, while N_{s1} and N_{s2} respectively correspond to number of turns per pole per phase for the main and auxiliary winding.

A. MMF Distribution

Since it is only the main winding that is connected to supply, let the balanced three phase main windings be excited by a balanced sinusoidal source expressed as:

$$i_k(t) = I_{m1}\sin(\omega t + \alpha_k) \tag{2}$$

where k = a, b, c; $\alpha_a = \alpha$; $\alpha_b = \alpha - 2\pi/3$; $\alpha_c = \alpha - 4\pi/3$, ω is the electrical angular speed of the current, and I_{m1} is the peak value of the main winding current.

It can be shown that the resultant MMF due to the winding set *abc* is:

$$F_{g1}(\theta,t) = F_{m1}\sin(\omega t - \alpha + \varphi_1 - p\theta) \tag{3}$$

where $F_{m1} = \frac{3}{2}N_{s1}I_{m1}$

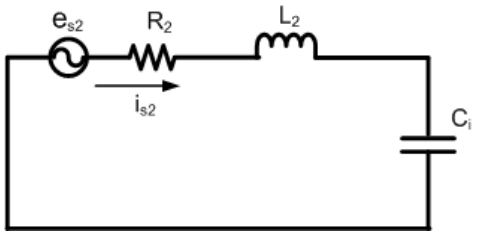

Fig. 2: Per phase representation of the auxiliary winding

Since the auxiliary winding *xyz* shares the same magnetic structure with winding *abc*, and magnetically coupled to the main winding *abc*, therefore, by transformer action, an emf e_{s2} is induced in the winding *xyz*. A simplified representation of the auxiliary winding in per phase is shown in Fig. 2. A leading current i_{s2} flow in the auxiliary windings; the magnitude and phase of which is largely determined by the impedance of the auxiliary winding *xyz* as influenced by the size of the capacitance attached to the winding *xyz*.

Since the windings *xyz* are assumed to be balanced, three phase currents I_{xyz}, with the current in each phase expressed by (4) will flow in the auxiliary windings.

$$i_k(t) = I_{m2}\sin(\omega t + \alpha_{ak}) \tag{4}$$

where k = x, y, z; $\alpha_{ax} = \alpha_a$; $\alpha_{ay} = \alpha_a - 2\pi/3$; $\alpha_{az} = \alpha_a - 4\pi/3$ and $\alpha_a = \tan^{-1}\left(\frac{X_2 - X_c}{R_2}\right)$

Similar to the main winding, it can be shown that the total MMF contribution due to the winding set xyz is:

$$F_{g2}(\theta,t) = F_{m2}\sin(\omega t - \alpha_a + \varphi_2 - p\theta) \tag{5}$$

where $F_{m2} = \frac{3}{2}N_{s2}I_{m2}$ gives the peak value of the MMF due to the auxiliary winding.

It is apparent from (3) and (5) that at an arbitrary instant in time, there are two MMF distributions along the airgap, and the resultant field is sinusoidally time variant and rotating at constant speed ω rad/sec. The total MMF developed by the currents in windings *abc* and *xyz* can be expressed as:

$$\begin{aligned} F_{gt}(\theta,t) &= F_{g1}(\theta,t) + F_{g2}(\theta,t) \\ &= F_{m1}\sin(\omega t - \alpha + \varphi_1 - p\theta) \\ &\quad + F_{m2}\sin(\omega t - \alpha_a + \varphi_2 - p\theta) \end{aligned} \tag{6}$$

B. Stored Energy

The reluctance rotor is usually designed to ensure a large variation of airgap permeance (saliency) with respect to the angular position. Due to this saliency, the airgap is not constant as for the case of any round rotor machine, but it is a function of the angular position θ and the rotor mechanical angle θ_{rm}. If the rotor pole arc is given as τ_p, the airgap function is expressed as [12, 13, 15]:

$$g^{-1}(\theta,\theta_{rm}) = m + n\cos 2p(\theta - \theta_{rm}) \tag{7}$$

where $m = \frac{1}{2}\left(\frac{1}{g_1} + \frac{1}{g_2}\right)$, $n = \frac{1}{2}\left(\frac{1}{g_1} - \frac{1}{g_2}\right)\sin\frac{p\tau_p}{2}$, $\theta_{rm}=\omega t+\delta$,

g_1 is the airgap at the pole face and g_2 is the airgap between poles as shown in Fig. 1.

This machine develops energy based on the change of magnetic energy when the rotor moves with respect to the stator MMF pattern. So, the stored energy in the magnetic circuit is expressed as [9, 11, 12]:

$$E = RL\int_0^{2\pi}\mu_o g^{-1}(\theta,\theta_{rm})F_{gt}{}^2(\theta,t)d\theta \tag{8}$$

When (6) and (7) are substituted into (8), the resulting expression expanded, integrated over the complete circumference, and carefully manipulated using trigonometry identities, some terms becomes zero, leaving terms which are either constant or dependent on the rotor angle δ. Wherefore, the energy stored in the magnetic circuit due to the combined MMF of the windings *abc* and *xyz* is obtained as

$$E = RL\mu_o\pi\begin{bmatrix} mF_{m1}{}^2 - \dfrac{nF_{m1}{}^2}{2}\cos 2(\alpha-\varphi_1+\delta) \\ +mF_{m2}{}^2 - \dfrac{nF_{m2}{}^2}{2}\cos 2(\alpha_a-\varphi_2+\delta) \\ -mF_{m1}F_{m2}\cos(\alpha-\alpha_a-\varphi_1+\varphi_2) \\ -\dfrac{nF_{m1}F_{m2}}{2}\cos(\alpha+\alpha_a-\varphi_1-\varphi_2+2\delta) \end{bmatrix} \quad (9)$$

In (9), only the terms that are dependent on the rotor angular position δ participate in the development of electromagnetic torque.

C. *Torque Equation*

The average electromagnetic torque developed is defined as the rate of change of the stored energy with respect to the rotor angular position, and it is expressed as:

$$T_{av} = p_r\frac{dE}{d\delta} \quad (10)$$

where E is the energy stored in the magnetic circuit, and defined for this machine by (9). Substituting (9) into (10), and solving, the average torque developed by the machine is obtained as:

$$T_{av} = p_r\mu_o\pi RL\begin{bmatrix} F_{m1}{}^2\sin 2(\alpha-\varphi_1+\delta) \\ +F_{m2}{}^2\sin 2(\alpha_a-\varphi_2+\delta) \\ +F_{m1}F_{m2}\sin(\alpha+\alpha_a-\varphi_1-\varphi_2+2\delta) \end{bmatrix} \quad (11)$$

Equation (11) can be simply expressed as:

$$T_{av} = T_{e1} + T_{e2} + T_{e3} \quad (12)$$

It follows from (11) and (12) that the torque developed by the machine configuration reported in this paper have three main components identified as T_{e1}, T_{e2}, and T_{e3}. The term T_{e1} clearly represents the torque contribution of the main winding. T_{e2} is similar to T_{e1}, and it is an additional component representing the unique contribution of the auxiliary winding and the capacitance injection. The effect of the capacitance on this torque component (T_{e2}) is clearly manifested in the peak value of the MMF as well as the angle α_a of (11). T_{e3}; the third component of the torque developed by this machine is as a result of the interaction of the two winding currents: main (I_{abc}) and auxiliary (I_{xyz}) currents. The second and the third torque components will only be developed when capacitor is connected to the auxiliary winding. Otherwise T_{e2} and T_{e3} will be set to zero, thus, the machine will only act as a standard synchronous reluctance machine. The additional torque components, T_{e2} and T_{e3} of (12) noticeably represent the influence of the magnetically coupled two three phase winding and capacitance injection, on the torque performance of the synchronous reluctance machine with simple salient rotor structure.

IV. FLUX DISTRIBUTION

The total airgap flux density at any position that contributes towards energy conversion is defined as

$$B_{gt}(\theta,t) = \mu_o F(\theta,t)g^{-1}(\theta,\theta_{rm}) \quad (13)$$

where F_{gt} is the total MMF at any position θ and instant t, derived and expressed by (6). g^{-1} is the inverse airgap function of a reluctance machine. Substituting (6) and (7) into (13), and simplifying using some trigonometrical manipulations, the total airgap flux density is:

$$B_{gt}(\theta,t) = \begin{bmatrix} B_{m1}\sin(\omega t-\alpha+\varphi_1-p\theta) \\ +B_{m2}\sin(\omega t-\alpha_a+\varphi_2-p\theta) \\ +B_{n1}(\sin(p\theta-\omega t-\alpha+\varphi_1-2\delta) \\ \quad +\sin(3\omega t-\alpha+\varphi_1-3p\theta+2\delta)) \\ +B_{n1}(\sin(p\theta-\omega t-\alpha_a+\varphi_2-2\delta) \\ \quad +\sin(3\omega t-\alpha_a+\varphi_2-3p\theta+2\delta)) \end{bmatrix} \quad (14)$$

where
$B_{m1}=\mu_o mF_{m1}$, $B_{m2}=\mu_o mF_{m2}$, $B_{n1}=½\mu_o F_{m1}$ and $B_{n1}=½\mu_o F_{m2}$
Equation (14) represents the time and space variations of total airgap flux densities produced by the currents in the two windings sets: abc and xyz. The flux density components B_{m1} and B_{n1} are the peak values of the flux density contributed by the main winding abc while, B_{m2} and B_{n2} are the peak values of those contributed by the auxiliary winding. These flux components in (14) excluding the third harmonic content, basically contribute towards the energy conversion.

For the typical experimental machine used in this work, some 3D plots showing the time and space variations of the airgap flux density components produced by the stator windings, for different capacitor and load angles are graphically illustrated in Figs. 3 and 4.

The plots of Figs. 3 - 5 were generated using (14), and the steady state stator winding currents obtained from experimental measurements on the prototype machine. It is easily observed from these figures that, the net flux in the stator of the machine with the configuration discussed in this paper is a rotating sine wave. With the different capacitor size considered, the flux density in the air gap keeps the same shape, and moves around the inner surface of the stator.

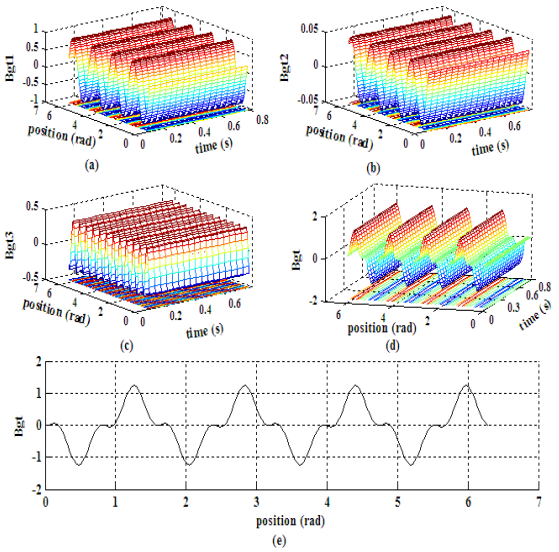

Fig. 3: 3D plots of the airgap flux density at δ=25° with capacitance of 15μF per phase (a) Airgap flux density due to the main windings *'abc'* (b) Airgap flux density due to the auxiliary windings *'xyz '*(c) Third harmonic content of the airgap flux density (d) Total airgap flux density (e) 2D-plot of total airgap flux density versus position

In Fig. 5, the variation of the airgap flux density as a function of the capacitance injected, and the load angle is shown. This along with the curves of Figs. 3 and 4 also revealed the contribution of the auxiliary winding and capacitance injection in the energy conversion ability of the machine. The details in terms of the torque magnitude is evaluated and shown in section V.

V. COUPLED CIRCUIT MODELING AND ANALYSIS

The two stator winding sets; *abc* and *xyz* are magnetically coupled, but, electrically isolated. Therefore, the two stator windings can be represented as a coupled circuit with two branches, each having separate resistance, and leakage reactance together with a common mutual reactance [9, 10]. The mutual component arises from the fact that the two sets of stator windings occupy the same stator slots. The branch of the coupled circuit representing the auxiliary winding is connected to a capacitor C with a reactance X_c. An approximate but derivable per phase equivalent circuit which illustrates the machine concept discussed in this paper is shown in Fig. 6.

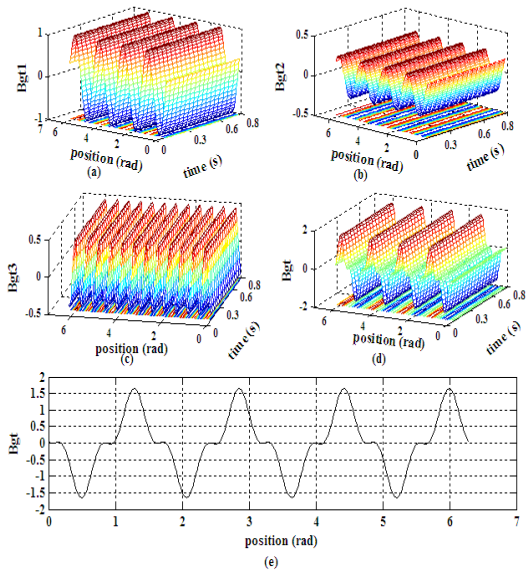

Fig. 4: 3D plots of the airgap flux density at δ=25°with capacitance of 75μF per phase (a) Airgap flux density due to the main windings *'abc'* (b) Airgap flux density due to the auxiliary windings *'xyz'* (c) Third harmonic content of the airgap flux density (d) Total airgap flux density (e) 2D-plot of total airgap flux density versus position

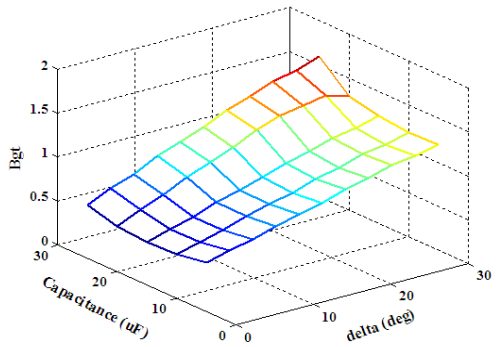

Fig. 5: 3D plot of the total airgap flux density as a function of capacitance and load angle

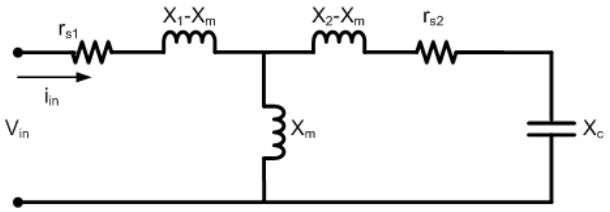

Fig. 6: Per phase equivalent circuit of a synchronous reluctance machine with dual winding and capacitance injection

Since the machine under consideration in this paper is of the salient rotor structure type, the effect of this rotor is manifested in the derivable equivalent circuit on the fact that, the synchronous impedance will vary with the saliency of the rotor of the machine. Assuming negligible resistance, it is defined as a function of the angular position δ of the direct axis of the rotor with respect to the axis of MMF, and is expressed as [15]:

$$X = \tfrac{1}{2}(X_d + X_q) + \tfrac{1}{2}(X_d - X_q)\exp(2\delta) \qquad (15)$$

where X_d and X_q are the steady state d and q axis reactance respectively, δ is the load angle of the machine and X_m in the figure is the mutual between the two windings. The coupled circuit of Fig. **6** along with (15) is used in the following sections to investigate the effect of the magnetically coupled, double stator winding and capacitance injection on the torque and power factor performance of the synchronous reluctance.

A. Input Impedance

Based on Fig. 6, the total per phase impedance of the machine $Z_{T\text{-}ph}$ is expressed as

$$Z_{T-ph} = (r_{s1} + jX_{L1}) + [jX_m // (r_{s2} + j(X_{L2} - X_c))] \qquad (16)$$

where X_{L1} and r_{s1} respectively represent the leakage inductance and resistance of the main winding, X_{L2} and r_{s2} represent the leakage inductance and resistance of the auxiliary winding and X_c is the reactance presented by the capacitor injected into the machine through the auxiliary winding.

To effectively illustrate the effect of capacitance value on the d- and q- axis reactances of the machine, we substitute, δ = 0, and δ = π/2 into (16) and obtain two equations which can be written in compact form as

$$Z_{d,q} = r_s 1 + j\left(X_{L1} + X_{d,q}\left(\frac{r_{s2} + j(X_{L2} - X_c)}{r_{s2} + j(X_{d,q} + X_{L2} - X_c)}\right)\right) \qquad (17)$$

Neglecting resistances, we obtain the effective d- and q-axis reactances X_d and X_q of the machine. To illustrate the effect of the capacitance on X_d and X_q, the reactances are plotted against capacitance as shown in Fig. 7. It is obvious in Fig. 7 that there are two resonant points, at $X_{c1}=X_d$ and $X_{c2}=X_q$. The latter has no practical value while the region in the vicinity of $X_{c1}=X_d$ is useful since a very high saliency ratio of about 170 is realized! Although a super high reactance ratio is obtained, it will be seen in the next section that a correspondingly high torque cannot be realized, but a very substantial improvement in power factor.

B. Impact of the scheme on Power Factor of the Machine

The power factor for the synchronous reluctance machine illustrated by the per phase equivalent circuit of Fig. 6 is evaluated using

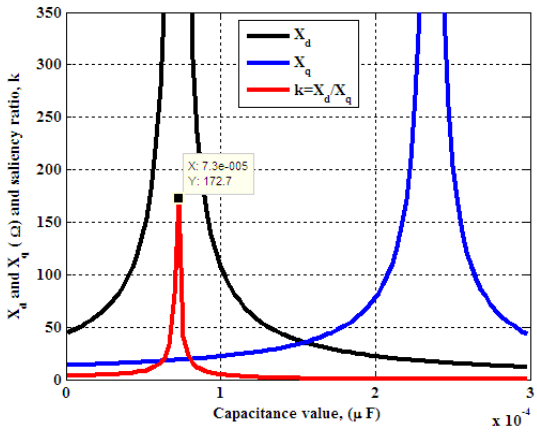

Fig. 7: Effective reactances X_d and X_q and saliency ratio versus capacitance

$$\cos\phi = R_{eq} \Big/ \sqrt{R_{eq}^{\ 2} + X_{eq}^{\ 2}} \qquad (18)$$

where R_{eq} and X_{eq} represent the effective resistance and reactance of the entire circuit of Fig. 6 when viewed from the main source. Equation (18) was arranged in a MATLAB environment and the power factor characteristics of the modified machine as determined using the coupled circuit method, in relation to the size capacitance at different load angle are shown in Fig. 8 and 9. It is observed from these figures that unlike the conventional reluctance machine of the same dimensions (with an estimated maximum power factor of 0.56), the machine with the new configuration offered a power factor of as high as 0.95. This is achieved by the presence of the auxiliary winding and capacitance injection, which influence the effective reactance of the machine. A 3D plot of the variation of the current with the load angle and capacitance is also shown in Fig. 9. While the equivalent circuit of Fig. 6, used in this analysis is an approximation, general trend in the plots of Fig. 8 taken for different load angles are the same. These plots showed that, the inherent power factor of the machine increase with increase in the size of capacitor attached to the auxiliary winding, and points of high power factor correspond to points of minimum current in the main winding.

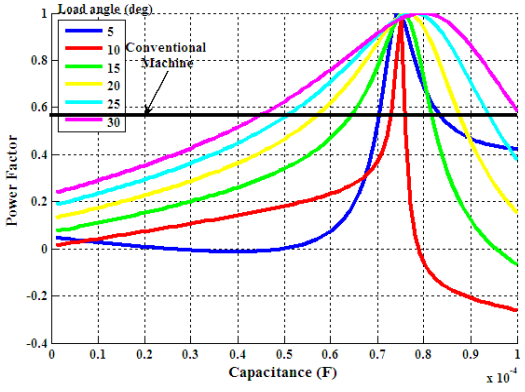

Fig. 8: Plot of power factor against capacitance at different load angles

C. *Impact of the Scheme on Torque of Synchronous Reluctance*

Given the theoretically predicted saliency ratio in section V-A, for machine with the configuration discussed in this

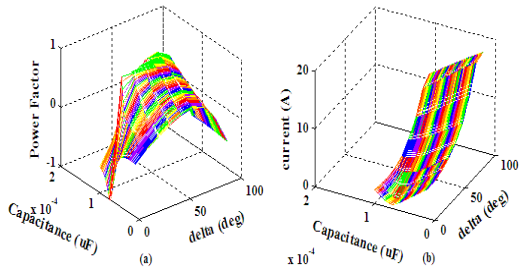

Fig. 9: 3D plots showing the variation of power factor and (b) 3D plots showing the variation of the main winding current, as a function of load angle and capacitance

paper, it is possible to obtain a very high torque, since the difference between the effective d- and q- axes reactance is very large, however it is not so. This is obviously explained by (19) which is the equation of torque as derived from the first principle in terms of delta for the machine:

$$T_{em} = \frac{3p_r V^2 (X_c - X_L)^2 (X_q - X_d)\sin 2\delta}{(X_q X_c - 2X_q X_L + X_L^{\ 2})(X_d X_c - 2X_d X_L + X_L^{\ 2})} \qquad (19)$$

Here, it is seen that if the leakage reactance is zero, the torque expression will be independent of the capacitive reactance, implying that its effect on torque is only to cancel out the leakage reactances. The variation of the torque as a function of the capacitance injected and the load angle is examined using (19) and results obtained are displayed in Fig. 10. The torque of the conventional synchronous reluctance machine was also determined, plotted and compared with that of the machine with magnetically coupled two stator windings and capacitance injection.

It is generally observed from these figures that, for every load angle considered, the torque of the machine slightly increase with the injection of capacitance and peaked at the point where capacitance $X_{c1} = X_d$. This initial increase is however found to drop (in most cases even to negative values), with a further increase in the capacitance beyond X_{c1}. This is obvious in the plot of Fig. 10 for $X_{c2} = X_q$. However, the slight increase of the torque with the capacitance injected is as a result of the changes in the ratio of direct axis to the quadrature axis reactance which resolves from the available flux within the machine.

It is obvious from these curves that for the machine with the parameters specified in Table 1, the relative improvement in torque is only evident at a load angle beyond 15°. Furthermore, this improvement increases with increase in load angle. High power factor were also seen to be achieved at the load angles that corresponds to the ones where torque improvement is identified.

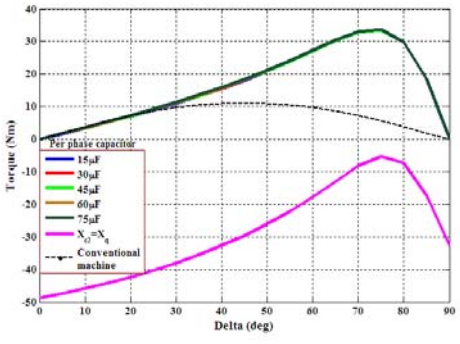

Fig. 10: Improvement in torque against delta at different capacitances

TABLE 1
MACHINE PARAMETERS

Parameter	Value
Airgap at pole face, g_1	0.25mm
Airgap between poles, g_2	12.0mm
Stack length, L	148.5mm
$N_{s1} = N_{s2}$	45
Voltage, V	150V
Frequency, f	50Hz
Rated main winding current	8.8A
Direct-axis reactance, X_d	43.31Ω
Quadrature-axis reactance, X_q	12.60Ω
Pole arc/pole pitch ratio	0.5
Stator outer diameter	188mm
Stator inner diameter	110mm

VI. CONCLUSION

An attempt using the simplified electromagnetic field approach and an approximate coupled circuit to provide an understanding of the operation, as well as the benefits of synchronous reluctance machine with magnetically coupled double three-phase stator windings and capacitance injection is presented. The analysis provides some insights into the power factor and torque performance of the machine, and the following conclusions are established.

- The airgap flux distribution of the machine obtained using the field approach showed that the net flux distribution of the machine is sinusoidal, and that the presence of capacitor in the auxiliary winding improved the energy conversion ability of the machine.
- The torque equations derived from the first principle, using the field approach revealed additional torque components contributed by the auxiliary winding and capacitance injection. This indicates that the output torque of this machine is higher than that of its equivalent conventional synchronous reluctance machine.
- Similarly, using an approximate equivalent circuit based on coupled circuit method, for machine of the same dimensions, a theoretical high value of saliency ratio of about 170 was predicted for the machine with magnetically coupled double three-phase stator windings and capacitance injection. Though the saliency ratio seems impractical, it justify why the calculated torque of the machine discussed in this paper is relatively higher than that of the conventional reluctance machine. For different capacitor size, the general trend of the torque versus delta plots was the same.
- Over possible operational range of load angles, two unique capacitor sizes at which the machine can operate at unity power factor is established. However, in practice the size of capacitor that can be used will be constrained by the ampere turn capability of the auxiliary winding.
- At points of improved power factor, the currents drawn from the main supply are low.
- With known advantages and special application areas of synchronous reluctance machine with simple salient rotor, the machine with magnetically coupled, double three-phase stator windings and capacitance injection should find acceptability due to its benefits.

REFERENCES

[1] Z. Wu and O. Ojo, "Coupled-circuit-model simulation and airgap field calculation of a dual-stator-winding induction machine," *IEE Proceeding- Electrical Power Application,* vol. 153, pp. 387-400, 2006, 2006.

[2] L. Hunt, "A new type of induction machines," *J.IEE,* vol. 39, pp. 648–677, 1907.

[3] A. Munoz, and T. Lipo, "Dual stator winding induction machine drive," *IEEE Transactions on Industry Applications,* vol. 36, pp. 1369-1378, 2000.

[4] R. Schriferl and C. Ong, "Six phase synchronous machine with ac and dc stator connections, part 1: Equivalent circuit representations and steady state analysis," *IEEE Transactions on Power Apparatus and Systems,* vol. PAS-102, pp. 2685-2693, 1983.

[5] E. Fuchs and L. Rosenburg, "Analysis of alternator with two displaced windings," *IEEE Transactions on Power Apparatus and Systems,* vol. PAS-93, pp. 1776-1786, 1974.

[6] M. Touma-Holmberg and K. Strivasta, "Double winding, high voltage cable wound generator: Steady state and fault analysis," *IEEE Transactions on Energy Conversion,* vol. 19, pp. 245-250, 2004.

[7] P. Franklin, "A theoretical study of the three-phase salient pole type generator with simultaneous ac and bridge rectified dc output-part 1." pp. 543-551, 1972.

[8] T. Kataoka and E. Wanabe, "Steady state characteristics of a current-source inverter/double wound synchronous machine for ac power supply," *IEEE Transactions on Industry Applications,* vol. 1A-16, pp. 262-270, 1980.

[9] A. S. O. Ogunjuyigbe, A. A. Jimoh and D. V. Nicolae, "Improving synchronous reluctance machine performance by direct capacitance injection through an auxiliary winding." pp. 1055-1060, 2007.

[10] E. Obe and T. Senjyu, "Analysis of a polyphase synchronous reluctance machine with two identical windings," *Electric Power System Research* vol. 76, pp. 515-524, 2006.

[11] O. Ojo, G. Dong and M. Omoigui, "Analysis of a synchronous reluctance machine with an auxiliary single phase winding," *IEEE Transactions on Industry Applications,* vol. 39, pp. 1307-1313, 2003.

[12] E. Spooner and A. Williams, "Mixed pole windings and some applications," *IEE Proceedings,* vol. 137, no. pt. B, pp. 89-97, 1990.

[13] H. A. Toliyat, S. P. Waikar and T. A. Lipo, "Analysis and simulation of five phase synchronous reluctance machines including third harmonic of airgap mmf," *IEEE Transactions on Industry Applications,* vol. 34, no. 2, pp. 332-339, 1998.

[14] P. Krause, *Analysis of Electric Machinery*: McGraw-Hill Book Company, 1986.

[15] L. A. Agu, L. U. Anih, O. Ojo *et al.*, "Novel synchronous reluctance machine with capacitance injection." pp. 1-8.